Comparison between X-ray tube based and synchrotron radiation based µCT

Oliver Brunke[a]*, Kathleen Brockdorf[b], Susanne Drews[c] , Bert Müller[c], Tilman Donath[d], Julia Herzen[d], and Felix Beckmann[d]
[a]phoenix|x-ray Systems + Services GmbH, Niels-Bohr-Str. 7, 31515 Wunstorf, Germany
[b]phoenix|x-ray Systems + Services Inc., 111 2nd Avenue N.E., St. Petersburg, FL 33701, USA
[c]Biomaterials Science Center, University of Basel, 4031 Basel, Switzerland
[d]GKSS-Research Center, Max-Planck-Str. 1, 21502 Geesthacht, Germany

ABSTRACT

Nowadays, X-ray tube-based high-resolution CT systems are widely used in scientific research and industrial applications. But the potential, convenience and economy of these lab systems is often underestimated. The present paper shows the comparison of sophisticated conventional µCT with synchrotron radiation-based µCT (SRµCT). The different aspects and characteristics of both approaches like spatial and density resolution, penetration depth, scanning time or sample size is described in detail. The tube-based µCT measurements were performed with a granite-based nanotom®-CT system (phoenix|x-ray, Wunstorf, Germany) equipped with a 180 kV – 15 W high-power nanofocus® tube with tungsten or molybdenum targets. The tube offers a wide range of applications from scanning low absorbing samples in nanofocus® mode with voxel sizes below 500 nm and highly absorbing objects in the high power mode with focal spot and voxel sizes of a few microns. The SRµCT measurements were carried out with the absorption contrast set-up at the beamlines W 2 and BW 2 at HASYLAB/DESY, operated by the GKSS Research Center. The range of samples examined covers materials of very different absorption levels and related photon energies for the CT scans. Both quantitative and qualitative comparisons of CT scans using biomedical specimens with rather low X-ray absorption such as parts of the human spine as well as using composites from the field of materials science are shown.

Keywords: X-ray tube CT system, synchrotron radiation-based CT, comparison, nanofocus X-ray tube, bone architecture, composite microstructure

1. INTRODUCTION

High resolution CT nowadays is a well established method for numerous industrial applications [1][2][3] as well as for a wide range of research areas [4][5]. For both fields the choice of the optimal method is strongly driven by many different factors like sample size and composition, required spatial and contrast resolution or scanning volume and time, etc.

For example in today's quality market, achieving the smallest feature recognition possible in the inspection process has become a higher priority than ever before. Due to complex geometries and miniaturization of many high reliability components in the automotive, electronics and aerospace industries, achieving this level of feature recognition has also become increasingly difficult. CT techniques are used to measure internal distances or the internal wall thickness of complex castings and areas which are often inaccessible for optical scanners or conventional tactile coordinate measurement machines. The CT volume data provides information for reverse engineering or first article inspection of the entire part by merging it with the CAD model to generate a variance map of both data sets [6][7][8]. Combined these capabilities contribute to early detection of process and product weaknesses therefore increasing yield and productivity.

*obrunke@phoenix-xray.com; phone +49 5031 172142; fax +49 5031 172299; www.phoenix-xray.com

Developments in X-Ray Tomography VI, edited by Stuart R. Stock,
Proc. of SPIE Vol. 7078, 70780U, (2008) · 0277-786X/08/$18 · doi: 10.1117/12.794789

Regarding high resolution computed tomography with voxel sizes of a few microns or even in the submicron range the state of the art benchmark is defined by CT setups which use synchrotron radiation for the X-ray source. Synchrotron radiation based CT was introduced in the 1980s by Bonse et al [9]. Nowadays it is a standard experiment for users from public research as well as industry at numerous Synchrotron laboratories worldwide. The main advantages of these setups are the highly collimated and almost parallel beam and the photon flux which is several orders of magnitude higher than for conventional X-ray sources. Due to this high flux monochromators can be effectively used to perform CT scans with monochromatic radiation at the desired energy level.

However, in recent years major steps in important hardware components like open microfocus or even nanofocus® X-ray tube technology (the later was commercially introduced the first time by phoenix|x-ray in 2001) on the one side and the development of highly efficient and large flat panel detectors (by e.g. GE, Perkin-Elmer, Varian or Hamamatsu) using CCD or CMOS technology on the other, allowed the development of very versatile and high resolution laboratory CT systems like the nanotom® (see next section) which are commercially available. Electromagnetic focusing of the electron beam allows generating X-ray beams with an emission spot diameter down to well below one µm which is essential for CT examination with voxels-sizes in the sub-micron range. These characteristics principally allow CT measurements which with respect to spatial resolution can compete with many absorption contrast setups at synchrotron radiation facilities [10]. The advantages of laboratory X-ray tube based setups like e.g. its accessibility, user-friendliness, cost effectiveness, large scanning area and thus comparably high scanning speed (especially for cone beam based systems like the nanotom®) are unfortunately still quite often not known or neglected. The purpose of this work is to show the potential of high resolution laboratory CT scanners as a powerful complementary approach, to support the costly, time consuming and complex examination at synchrotron facilities. In the following the comparison of datasets obtained with both, an absorption contrast SRµCT setup and a state of the art high resolution cone beam laboratory scanner will show the unique properties of both approaches. The advantages (and limitation) of both methods are shown at several example specimen with high and low absorption characteristics. It covers the materials science sector as well as the biomedical world.

2. THE CT SYSTEMS

2.1 nanotom®: a high resolution and versatile laboratory CT system

The nanotom® was introduced in 2006 by phoenix|x-ray in order to cover the growing demands for a compact laboratory CT system for spatial resolutions which could up to then only be reached by synchrotron radiation based setups on the one hand. On the other it should to give the user highest flexibility for applications in fields such as materials science, micro mechanics, electronics, geology, and biology to name a few. Therefore, it is particularly suitable for examination of sensors, complex mechatronic samples, microelectronic components as well as for material samples such as synthetic materials, ceramics, sintered alloys, composite materials, mineral and organic samples.

In order to cover the widest possible range of samples the system is equipped with the first commercially available 180kV/15W high power nanofocus® (HPNF) tube. This source can be operated in four different modes. On the one hand in the so called nanofocus® mode it provides an X-ray spot size of down to approximately <0.9 µm which can be used for highest resolution CT scans with submicrometer voxelsize. Due to the penumbra effect the spot size predominates the image sharpness for extreme magnifications (for details see e.g. [11]). In Fig. 1 (a) the resolution capability of the high power nanofocus® source is demonstrated. It shows that the 0.6 µm structure (line width) of the so called JIMA test pattern (designed by the **J**apan **I**nspection Instruments **M**anufacturers' **A**ssociation for testing high resolution X-ray equipment [12]) can clearly be resolved with more than approximately 20% of the CTF. Fig. 1(b) shows that for isolated structures of high absorbing material on a low absorbing substrate it is even possible to detect details of 0.5 µm size and below. The limit for this so called detail-detecability for the HPNF tube lies at about 200 – 300 nm.

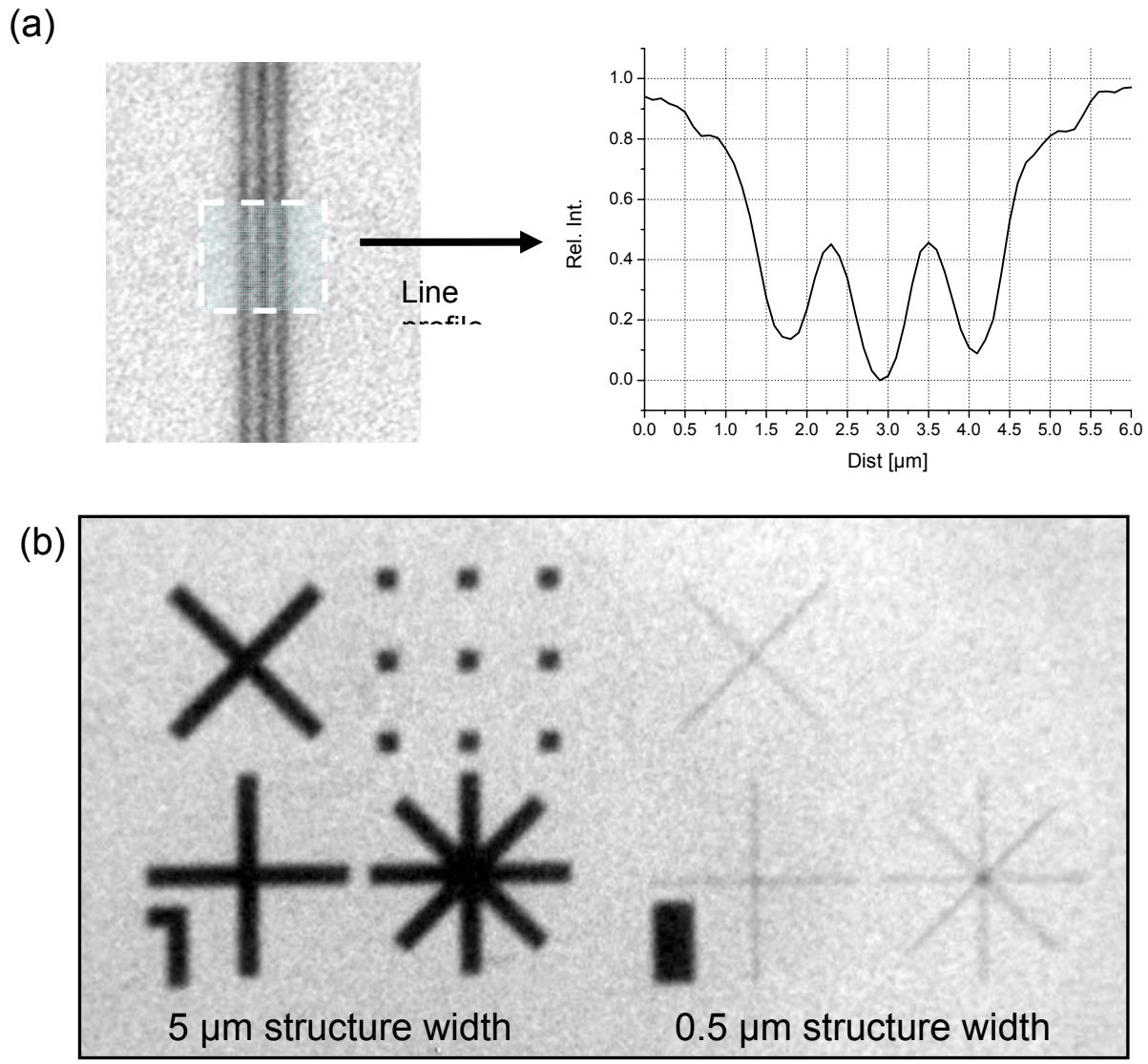

Fig. 1: X-ray images of test patterns showing the capabilities of resolution and detail detectability of phoenix|x-ray's high power nanofocus® tube. In (a) the 0.6 µm line pair structure of the JIMA test pattern is clearly resolved. (b) shows the capabilities of the tube to resolve structures which are as small as 0.5 µm and below.

In the high power mode (up to 15 Watts at the target) on the other hand it has enough penetration power to examine high-absorption samples like copper steel or tin alloys and thus allowing e.g. the analysis of new connection systems for electronic devices or high absorbing geological samples, etc. The tube is equipped with a so-called transmission type target. This means the target is a thin layer (a few microns) of W or Mo which has been sputtered on the Be exit window which is hit by the focused electron beam. For the transmission geometry the X-rays are emitted in the same direction as the incoming electron beam.

On the detection side a 5-megapixel flat panel CMOS detector with a GOS scintillator deposited on a fiber optic plate is used. The pixel size of 50 µm and a 3-position virtual detector (i.e. 360 mm detector width) give rise to a wide variety of experimental possibilities. To avoid any potentially negative influence of vibrations or thermal expansion, tube, detector and manipulator are mounted on a granite structure. Furthermore, special materials and construction details for e.g. the

tube mounting are used to minimize the variation of the focal-spot/detector distance during a scan. In addition, minimal vibrations of the system are suppressed by air bearings of the rotation unit.

For reconstruction of the volume data phoenix|x-ray uses a proprietary implementation based on Feldkamps cone beam reconstruction algorithm [13]. The reconstruction software contains several different moduls for artifact reduction (e.g. beam hardening, ring artifacts, drift compensation) to optimize the results. In Fig. 2 the effect of the ring artifact suppression method is shown. In the figures two identical cross sections of a cortical bone sample (human bone) scanned with the nanotom® at 90 kV and 150 µA and 1.8 µm voxelsize are shown. The original study was performed by M. Dalstra et al using the SRµCT setups at HASYLAB/DESY. The study was performed to quantitatively evaluate the remodeling process in osteoporotic cortical bone [14]. For quantitative analysis of the datasets it is essential to minimize the artifacts in the reconstructed volume. As it can be seen in Fig. 2, the approach implemented by phoenix|x-ray effectively eliminates the ring artifacts and therefore a further quantitative analysis could also be performed on the nanotom® CT datasets as it was done with the results of theSRµCT scans. One remarkable result of the shown nanotom® data is the high contrast resolution which even allows a separation of the different density phases in the bone.

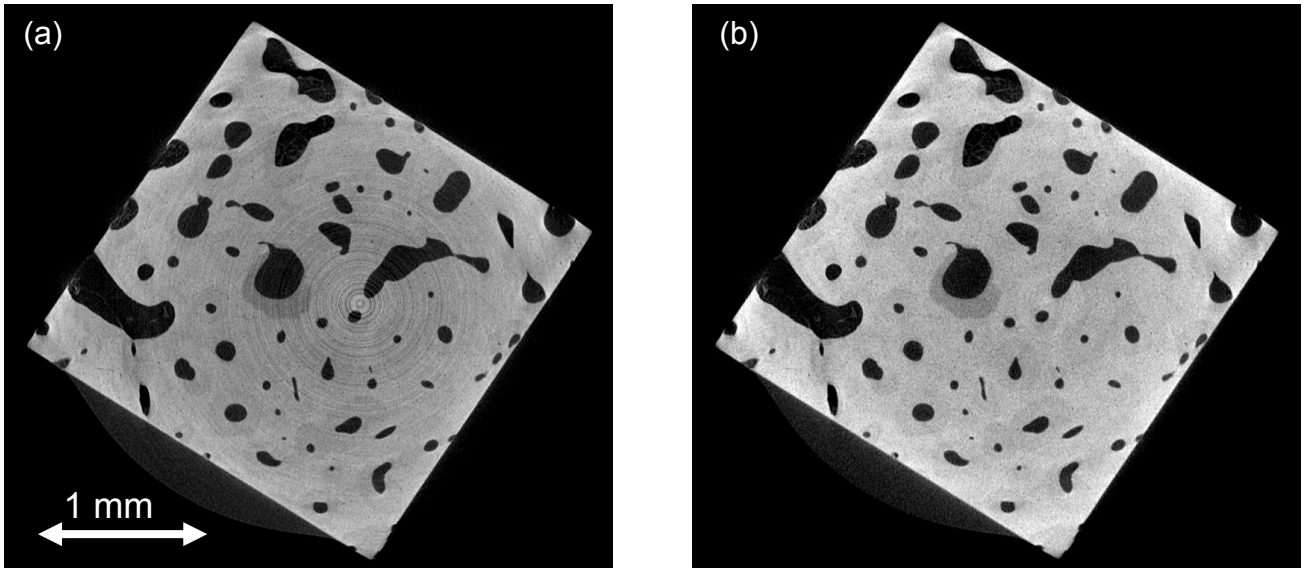

Fig. 2: Cross section of cortical bone sample scanned with the nanotom®. Due to an effective ring artifacts suppression a segmentation of the different phases in the bone structure becomes possible.

2.2 The Synchrotron CT setup

The SRµCT measurements were carried out at the 2nd generation storage ring DORIS III at HASYLAB/DESY in Hamburg/Germany. Two different beamlines have been used. For specimen with lower absorption coefficients like e.g. biomaterials polymers or ceramics the CT setup was installed at the beamline BW2 using photon energies in the range of 8 to 24 keV. For the investigation of larger samples and for samples consisting of stronger absorbing elements the apparatus was modified and installed at the high-energy beamline HARWI-II, operated by GKSS-Research Center Geesthacht/Germany, for the use of higher photon energies ranging from 20-250 keV. The technical description of the beamline is given in [15]. Especially for the investigation of high absorbing samples in the field of materials science, e.g. studying the plastic flow in friction stir welds, and medical application, e.g. implant material in bone, the use of higher photon energies becomes mandatory. The setup used for absorption-contrast microtomography is presented in detail in [16]. It consists of a 2-dim. X-ray detector and a sample manipulator stage. The sample manipulator provides both for the rotation and for the lateral positioning of the specimen. The incident X-rays are converted into visible light (scintillator: $CdWO_4$ single crystal, thickness 200µm - 1000µm) which then is projected onto a CCD camera (KX2, Apogee Instruments, Inc.; 14 bit digitalization at 1.25 MHz, 1536 x 1024 pixel) by an optical lens system. The spatial resolution limit for CT examination at both beamlines is approximately 2 µm. Currently, a new tomography instrumentation dedicated for beamline HARWI-II is under construction and will become operational in the fist half of

2009. By including new CCD cameras with 16 bit digitalization together with a new sample manipulator stage based on air bearing the density resolution and the troughput of the system will be increased.

For absorption-contrast microtomography typically a set of 720 radiograms at different sample rotations equally stepped between 0 and 180° were taken. The tomographical reconstructions are calculated by using the backprojection of filtered projection algorithm.

3. SAMPLES AND SCANNING PARAMETERS

Three different sample types have been chosen to be studied by SRμCT as well as high resolution conventional CT. Identical regions of the specimen described in the following have been scanned by both systems. In order to allow a quantitative comparison, the resulting volume data had to be registered to each other using either a software described also in this proceedings in [17] or VGStudio MAX 2.0 by Volume Graphcis in Heidelberg/Germany.

3.1 Sample 3: Cu/Al_2O_3 catalyst

Impregnation of pre-shaped metal oxide particles is one of the most applied preparation procedures of industrial heterogeneous catalysts. Different mathematical descriptions of the impregnation step have been developed. However, radial profiles have been seldomly measured in practice. One recent report shows the SRμCT datasets used for the present study [18]. Cu/Al_2O_3 catalysts, differently impregnated with $CuCl_2$-solution as described in ref. [18] and using alumina pellets of the same shape and size, were investigated. For the present study a cylindrical porous Al_2O_3 catalyst (3.3 mm diameter, 4 mm height) was immersed for 1 min in the impregnation solution. This sample was used to evaluate the contrast resolution of the nanotom®. One goal was to find out if as show in [18] for the SRμCT scans the position of the $CuCl_2$ diffusion front can be identified also with the laboratory CT system. Furthermore the fine grains of the specimen allow a qualification of the spatial resolution capabilities of the nanotom®.

3.2 Sample 2: Sintered Ti6Al7Nb

This alloy especially interesting as potential material for bone implants. In a GKSS research project the potential of this material class for medical application is evaluated. Goal of the CT scans is to analyze the 3D morphology of sintered porous Ti6Al7Nb. For the CT examinations four cylindrical specimen (3.5 mm diameter, 5 mm in height) have been produced from spherical Ti6Al7Nb particles. The particle diameter was as follows: sample (a): 45-75μm, sample (b): 75-90μm, sample (c): 90-125 μm and sample (d): 180-250 μm. The high absorbing Ti6Al7Nb samples have been scanned to demonstrate the capabilities of the laboratory system at higher acceleration voltages. It should be shown that within a rather short scanning time high resolution CT datasets of high absorbing materials can be obtained with the nanotom®.

3.3 Sample 1: Part of a human vertebra

Human spine on the one hand allows the upright gait one of the most important achievements of human beings, on the other hand especially in the western nations it often is held responsible for a large amount of diseases and consequently an enormous economic damage. Therefore the interest in morphology of physiologic and pathologic spine is increasing. One goal of the study was to make visible the bone-cartilage interface, where degenerative and inflammatory diseases have their origin. A special interest lies in the subchondral bone with its different calcification. More details of this work can be found in [17].

The specimen in hand was harvested out of the lumbar region of a juvenile human body. It consisted of two vertebral bodies, the intermediate intervertebral disc and the anterior and posterior longitudinal ligament. The vertebral arch was cut off using a band saw. Afterwards it was embedded in PMMA. The embedded samples were cut into 4 quarters. The sample named MA_BE is one of these quarters and had a maximal diameter of 1.3 cm.

For the present study the spine sample was interesting due to two reasons. On the one hand there is a strong difference in X-ray absorption coefficient for bone and cartilage. Therefore it is a good example to observe the influence of beam hardening for CT scans with polychromatic sources in contrast to monochromatic SRμCT. Furthermore it can be used to test the contrast resolution of the nanotom® due to the small absorption contrast difference between cartilage and the embedding matrix.

3.4 Overview of the CT parameters

An overview of the parameters which have been used for the nanotom® and the SRμCT system are shown in the tables one and two, respectively.

Table 1: Parameters of the nanotom® scans

Sample	Sample 1: Cu/Al203	Sample 2: Ti6Al7Nb (sample d)	Sample 3: Vertebra MA_BE
Acceleration Voltage	60 kV	100 kV	80 kV
e- beam current	240 μA	60 μA	180 μA
Tube operation mode	1	0 (High Power)	0 (High Power)
X-ray filter	0.1 mm Cu	0.5 mm Cu	None (Be exit window)
Focal spot size	< 2 μm	< 3 μm	< 3.5 μm
Voxel size	2.5 μm	4.5 μm	10 μm
Scanning volume	5x5x4.5 mm^3	5x5x4.5 mm^3	20x20x15 mm^3
Angular increment	0.12 °	0.36°	0.3°
Scanning time	160 min	20 min	80 min

As it can be seen in table 1, the tube of the nanotom® was not operated in the nanofocus® mode (mode 3) for the presented test samples. The size of the test samles physically limits the achievable magnification and thus voxelsize for scanning the complete sample for both systems (laboratory CT and SRμCT scans) and thus it was not necessary to use the nanofocus® mode. Results with subμm voxelsize and nanofocus® mode are e.g. shown in [11] or [10].

Table 2: Parameters of the SRμCT scans

Sample	Sample 1: Cu/Al203	Sample 2: Ti6Al7Nb (sample d)	Sample 3: Vertebra MA_BE
Beamline	BW2	HARWI-2	HARWI-2
Photon Energy	18 keV	65 keV	28 keV
Spatial Resolution (10% MTF)	4 μm	13.5 μm	13.9 μm
Voxel size	2.3 μm	2.7 μm	6.8 μm
scanning volume	3.5x3.5x2.3 mm^3	4.1x4.1x2.7 mm^3	20x20x3 mm^3
Angular increment	0.25 °	0.25°	0.25 °
Scanning time	160 min	90 min	180 min

The tables indicate one obvious advantage of the laboratory scanner. The achievable throughput (i.e. sample volume per time) is between 4 and 10 times higher for the nanotom®. This is mainly attributed to the fact that the cone beam geometry of the laboratory CT system covers a much larger scanning area than the parallel beam geometry of the SRμCT setup. The much lower flux of the X-ray tube is partly compensated by the comparably large detector pixel size (50 μm) and the high quantum efficiency of the flat panel detector. For the SRμCT setup it has to be noted that at the performed scans most of the scan time is used for alignment and calibration to obtain a high spatial and density resolution in the tomogram. The comparison of the actual results is given in the next section.

4. RESULTS AND DISCUSSION

In order to allow a direct and quantitative comparison of the datasets obtained by the two different setups first of all the datasets had to be aligned to each other. Sample orientation and position can obviously be very different for two scans of the same specimen. In order to allow a best fit registration the first step for the registration is a manual alignment using either (a) the software tool developed by Beckmann et al. described in [17] or (b) VGStudio MAX 2.0. Sample 3 was registered using method (a). For the samples 1+2 method (b) was chosen. For this method one first of all loads both datasets into VGStudio. Now prominent features (like larger high absorbing particles) are identified in both datasets to allow an easy manual pre-registration by shifting and rotating. Finally, a best fit algorithm is used to get the optimal registration of the datasets.

4.1 Cu/Al_20_3 catalyst

Sections of the CT datasets of the Cu/Al_20_3 catalysts are shown in Fig. 3 for the nanotom® scan on the left (a), for the SRμCT scan on the right, respectively. Looking at values for voxelsize and 2D resolution of both scans in the tables 1 and 2 (for the case of the nanotom® with a spot size which is below the voxelsize a 2D resolution close to the value given for SRμCT scan can be estimated) a comparable spatial resolution for the CT datasets can be expected. Both the 3D rendered image and especially the part of the cross section below clearly shows that the difference in spatial resolution of the scans is below 0.5 μm. Gaps between the grains down to 3-4 μm can be identified in both scans.

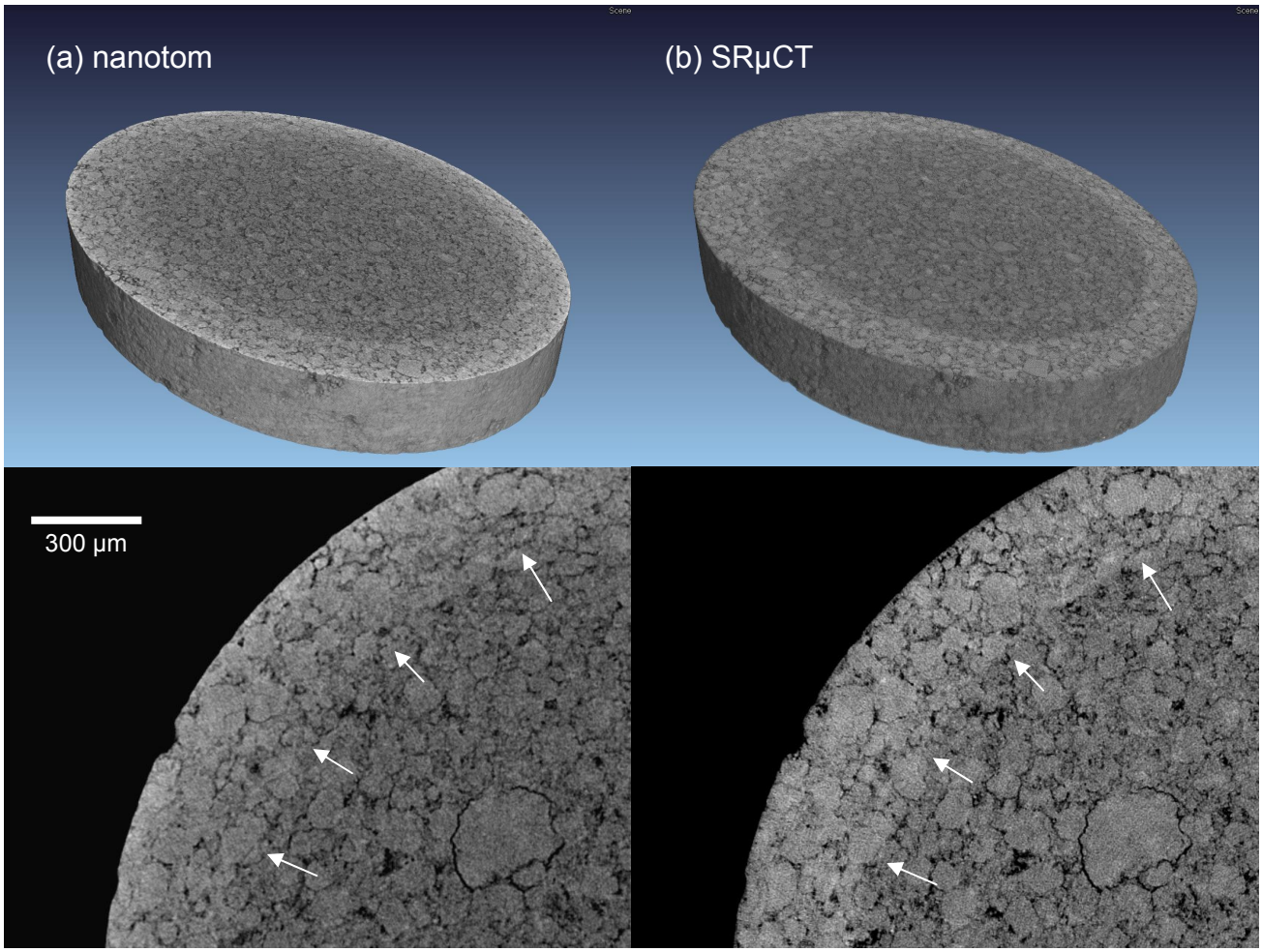

Fig. 3: Comparison of the CT results of the Cu/Al_2O_3 specimen. In both scans the outer ring like zone (white arrows) which has been infiltered by the CuCl can be observed. Whereas the spatial resolution appears very similar, the border of this zone is more obvious in the SRμCT scan due to the superior contrast resolution.

The images indicate also a comparable data quality with respect to ring artifacts (almost no such artifacts can be found) and signal to noise ratio.

One major goal of the CT examination of the Cu/Al_2O_3 specimen was to measure how deep the $CuCl_2$ has diffused into the porous ceramic matrix after different immersion times. As it can be seen in Fig. 3(b) the higher absorbing Cu can easily be found in the SRμCT datasets (the ring like structure at outer part of the cylinder) and a sharp end of the diffusion front can be identified. In case of the nanotom® dataset (a) it is obvious that also with the polychromatic X-ray source of the nanotom® it is possible to separate the Cu filled outer part of the specimen from the inner Cu free section. However, a small decrease in absorption coefficient from the border to the center of the sample can be found which can be attributed to beam hardening. This artifact is also referred to as cupping effect. A stronger pre-filtering of the source spectrum and/or additional software filters as described in the next section could further reduce this effect.

The comparison of the absorption coefficient histogram (Fig. 4) reveals further interesting aspects. As expected the absorption coefficient calculated from the nanotom® scan deviates from the SRμCT scan. This is no surprise as for polychromatic sources the assumption of the classical logarithmic absorption law is just a first order approximation (see e.g. [19]).

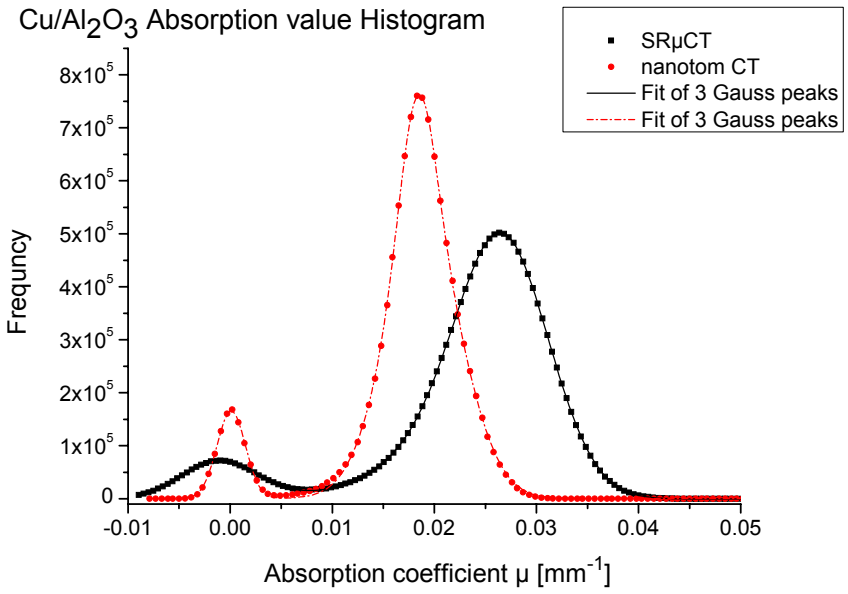

Fig. 4: Histogram for the absorption values of the CT datasets of the Cu/Al_2O_3 sample. In the SRμCT data the material peak more obviously contains to phases. Thus the plot confirms the interpretation of the images in Fig. 3.

Three Gaussian curves have been fit to both datasets. The result of the parameters fits are given in table 3. The values show a slightly better S/N of the nanotom® scan (smaller width of the peaks) but also the advantages in the contrast resolution of the SRμCT scan due to the monochromatic source (better separation of P2 and P3).

Table 3: Parameters of the Gaussian fits for the absorption value histogram shown in Fig. 4

	P1 Center	P1 Width	P2 Center	P2 Width	P3 Center	P3 Width
nanotom®	0.0001	0.003	0.017	0.007	0.019	0.004
SRμCT	-0.0002	0.007	0.021	0.013	0.027	0.009

4.2 Sintered Ti6Al7Nb particles

Out of the three examples this specimen showed by far the highest absorption behavior. Therefore in order to achieve proper penetration of the sample and an optimal scan result it was necessary to use relatively high acceleration voltages (100 kV) for the X-ray tube and also a high photon energy (65 keV) for the SRμCT measurement. In order to protect the lens system of the current absorption contrast SRμCT setup at higher photon energies a thicker (1mm) $CdWO_4$ crystal has to be used. On the one hand this has the advantages to increase the quantum efficiency of the setup, on the other the thicker screen limits the resolution for such scans as information is smeared out on the scintillator. Therefore even if the voxelsize for the SRμCT dataset is a factor of about 1.7 smaller than for the nanotom® data, the achieved spatial resolution is better for the laboratory scanner as it is shown in Fig. 5.

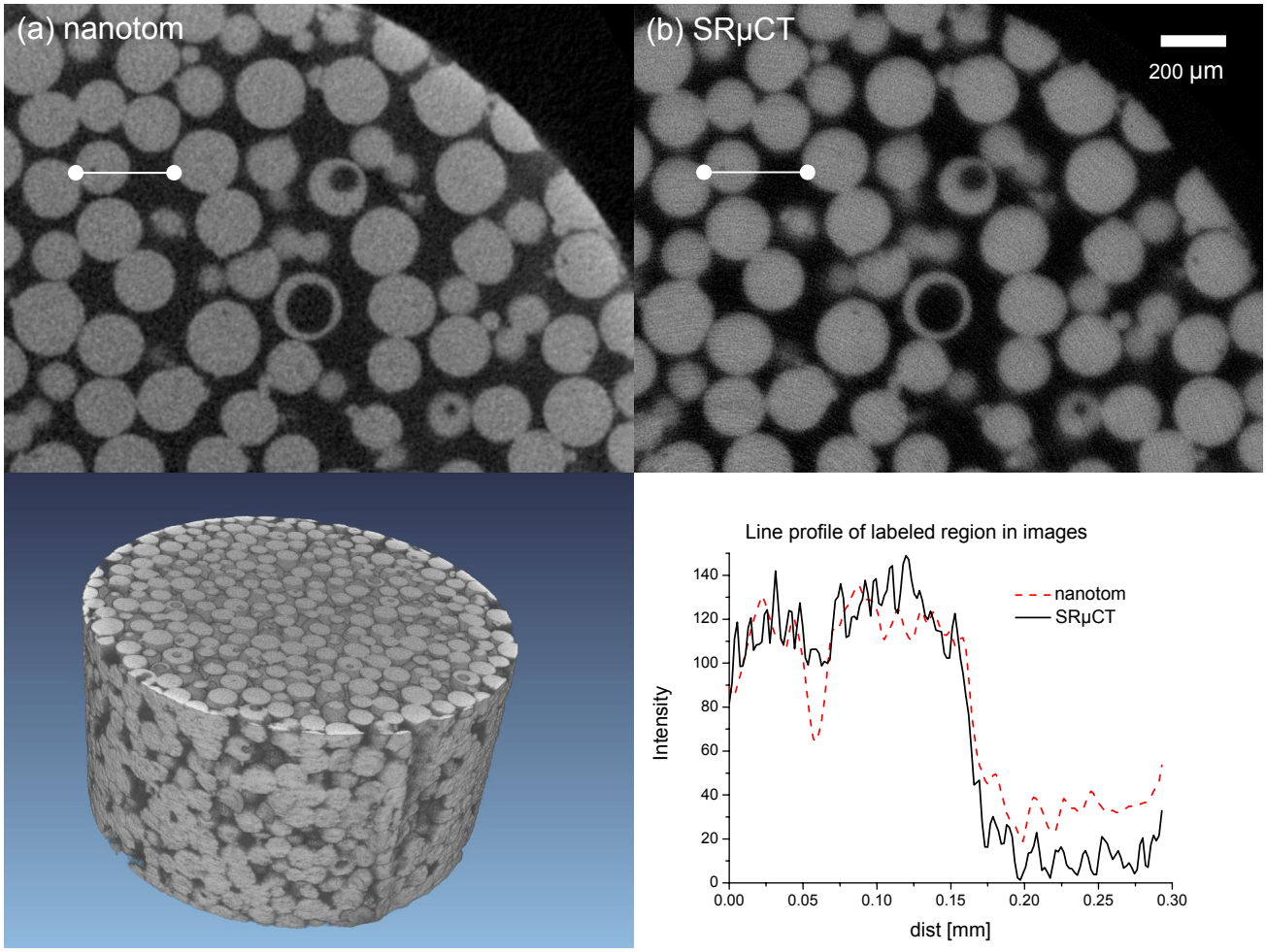

Fig. 5: CT results of the Ti6Al7Nb scans. The line profile confirms the higher resolution of the nanotom® scan.

A direct comparison of a line profile clearly shows the higher spatial resolution of the tube based scan data. In the future the setup at HASYLAB will use mirror system to protect the optical lenses from the higher harmonics of the direct beam thus allow to implement thinner scintillator crystals. Therefore an improved spatial resolution also for higher energies is expected.

With respect to signal to noise ratio and ring artifacts the lab data is slightly better than the SRμCT data as it can be derived from the absorption value histograms. On the other hand the nanotom® data again shows apparent higher absorption values at the outer edge of the sample due to beam hardening. However for this class of specimen which only contain one material phase this is not critical for quantitative morphology analysis methods. Typical tasks like the

determination of 3D pore or particle size distribution or the connectivity of the pore networks are e.g. described in [20] or [21].

4.3 Vertebral bone

A comprehensive comparison of the SRμCT dataset with data from conventional laboratory CT system is presented elsewhere in this proceedings [17]. However, a few aspects should also be described here, as this is a good example for the very wide class of specimen containing material with strong differences in X-ray absorption coefficient.

From the scan parameters a comparable spatial resolution can be expected for the scans. The exemplary analysis of the datasets shown in Fig. 6 confirms this assumption. Both, the cross-sectional images as well as the line profile show a very good agreement with respect to spatial resolution. The size of the smallest detectable details in both datasets is roughly 10-12 μm.

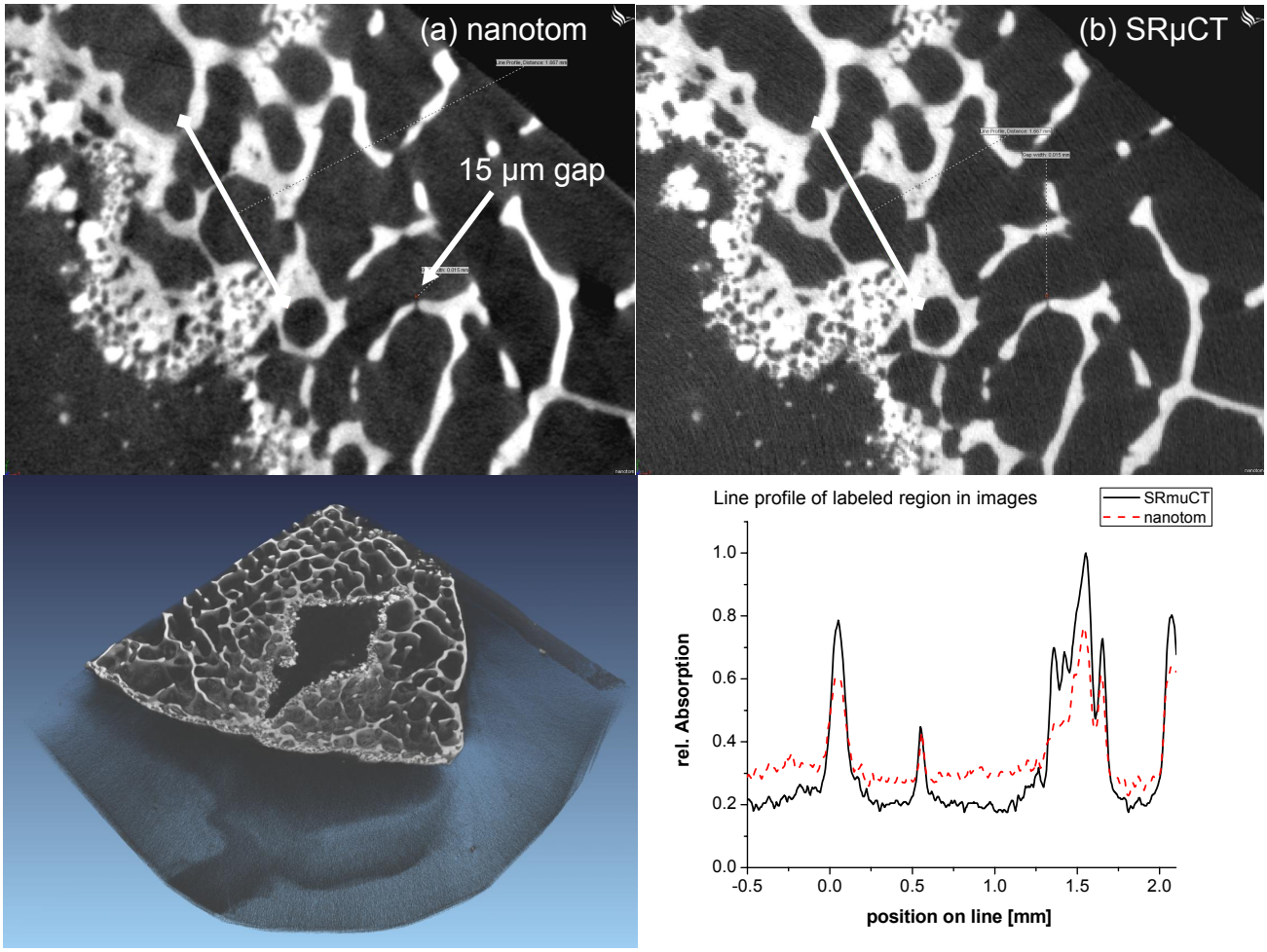

Fig. 6: Cross sections from the CT datasets of the vertebral bone. The region of the line profile is given in the image.

From the cross section images it can be seen that the SRμCT data shows slight rings which can not be found in the nanotom® scan. On the other hand the effect of the polychromatic source can be seen in Fig. 6(a). The low absorbing soft tissue contains dark (apparently low absorbing) areas the high absorbing bony tissue. These so called streak artifacts can have two reasons: beam hardening and scattered radiation (Compton scattering). Scattering obviously can occur for both source types. However, for the X-ray energies used in this work the dominant reason for streak artifacts is beam hardening and the streaks are more obvious in the nanotom® scan. Nonetheless due to scattering they can also be found (much less pronounced) in the SRμCT data. Beam hardening effects can be reduced with algorithms implemented in the reconstruction software or by pre-hardening the source spectrum using metal sheets from e.g. Al, Cu, Sn or even Pb depending on the used X-ray energies. The effect of numerical beam hardening correction and pre-hardening is shown in

Fig. 7. The cross-sections are taken from a CT dataset of a human jaw embed in PMMA scanned with the nanotom® at 100 kV and 400 µA. The sample was prepared and provided by M. Dalstra, University of Aarhus, Denmark. For the unfiltered scan (a) typical streak due to beam hardening can be found at the edges of jaw bone. After applying software beam hardening correction on the same dataset the streaks are cleary reduced (b). A filtering on the source spectrum with 0.1 mm of Cu gives the best result for this example. The artifacts are almost completely suppressed.

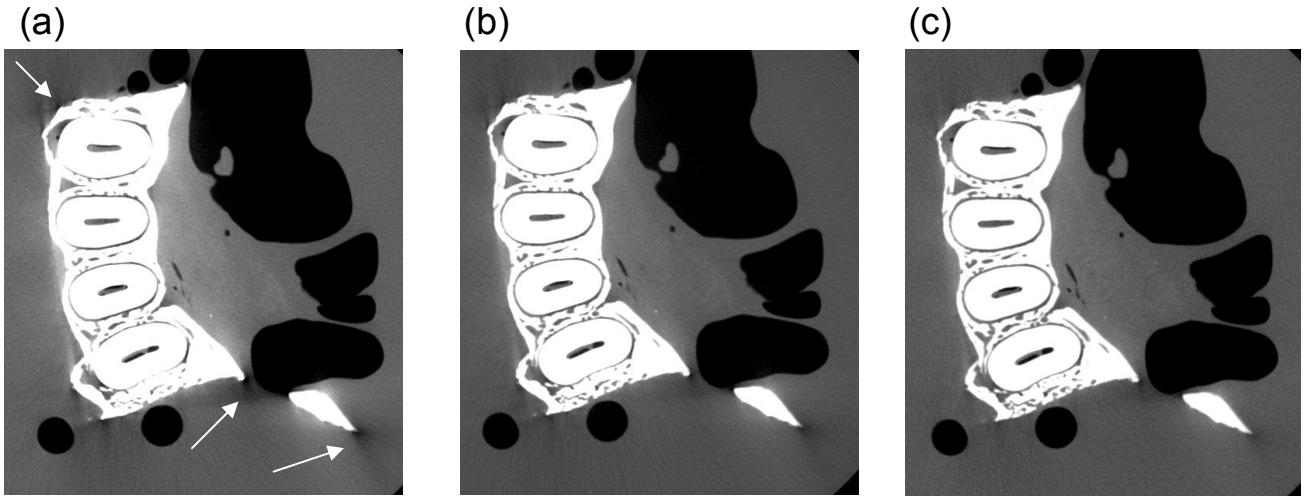

Fig. 7 Influence of beam hardening for a polychromatic source shown at a cross sectional image of a human jaw embedded in PMMA. (a) no beam hardening compensation (b) software compensation (c) prefiltering of the spectrum

5. SUMMARY AND OUTLOOK

In the present study aimed to show a comprehensive comparison of CT scans obtained with a commercial high end CT scanner with a nanofocus® X-ray tube and a absorption contrast synchrotron radiation based CT setup. Three samples with different absorption characteristics (a porous Al_2O_3 catalyst, sintered Ti6Al7Nb and part of human vertebra) have been scanned in a voxel size range between 2.3 and 10 µm. The chosen specimens are good examples for typical applications of both systems. In order to allow a direct and easy comparison of the results, the scan data has been registered to each other by a best fit algorithm. The analysis of the scans reveals that the nanotom® gives excellent data quality which in many cases can even compete with SRµCT data. For the shown examples the spatial resolution and also the signal to noise ration of the two systems was absolutely comparable. As the resolution limit of the current SRµCT setup at HASYLAB/DESY is limited to 2µm, it was not possible to compare nanotom® data with subµm voxelsize to corresponding SRµCT data right now. The next step will be a comparison of nanotom® data at the resolution limit of the system which is below 0.9 µm with the data from the next generation SRµCT setup at the new third generation source PETRA III at DESY which will be available in 2009.

In total the major advantages of the laboratory scanner are its large field of view, large scanning volume, high penetration power due to the 180kV tube, scanning speed (scanned volume per time), ease of use and overall cost effectiveness. The synchrotron radiation CT on the other hand provides an excellent contrast resolution, precisely adjustable monochromatic radiation and therefore no beam hardening artifacts. In conclusion state of the art conventional high resolution CT scanners like the nanotom® by phoenix|x-ray can adequately support and complement research projects where high quality CT data is required. Due to its flexibility the nanotom® can be used for both, extreme high resolution scans with subµm voxelsize of small samples on the one side or also fast scans of high absorbing (or larger) specimen using the high power mode on the other. Thus an ideal situation for such projects is to use both systems. For subµm scans or studies where a lot of samples have to be scanned the nanotom® will be used. Whereas for situations in which optimal contrast resolution or artifact free data is needed, the synchrotron radiation based CT would be the system of choice.

Acknowledgments

We thank DESY for providing the photons at the storage ring DORIS-III and the operation of beamline BW2. Thank also goes to J.-D. Grunwaldt, Technical University of Denmark, Lyngby, Denmark, for providing the Al_2O_3 sample. For the sintered TiAlNb particles we thank F. Feyerabend and R. Willumeit, GKSS. For the bone samples presented in Figures 2 and 7 we thank M. Dalstra and P.M. Cattaneo, University of Aarhus, Denmark.

REFERENCES

[1] Roth, H. Mazuik B., "What you can't see can hurt you", Quality Test and Inspection, 5, (2003)
[2] Moller – Gunderson, D., "When 2D X-ray isn't enough" SMT , 8, (2007).
[3] Nier, E., Roth, H., "Analysis of Crimp Interconnections by Microfocus Computed Tomography" QZ, 9, 916-918 , (2003).
[4] Bonse, U. (Editor.), "Developments in X-Ray Tomography IV" SPIE, Wellingham WA, (2004).
[5] Bonse U., (Editor.), "Developments in X-Ray Tomography V", SPIE, Wellingham WA, (2006).
[6] Obrist, A. et al., "First Article Inspection Based on Industrial X-ray Comuted Tomography", Materials Testing and Research, International Conference, Nuremburg, 177-180, (2001).
[7] Brunke O., "Dimensionelles Messen mit hochauflösender 3D-CT", QZ, 62-64 (2008).
[8] Suppes, A., Neuser, K., „Metrology with µCT: precision challenge" in Developments in X-ray Tomography VI, edited by Stuart Stock, Proceedings of SPIE Vol. 7078, (2008)
[9] Bonse U., Busch F., „X-ray computed microtomography (µCT) using synchrotron radiation (SR)., Prog. Biophys. Mol. Biol., 65(1-2), 133-169 (1996)
[10] Withers, P., "X-ray nanotomography", Materials Today, 10(12), 26-34 (2007)
[11] Brockdorf, K. et al., "Sub-mcron CT: visualization of internal structures" in Developments in X-ray Tomography VI, edited by Stuart Stock, Proceedings of SPIE Vol. 7078, (2008).
[12] Japan Inspection Instruments Manufacturers' Association, http://www.jima.jp
[13] Feldkamp, L.A., Davis, L.C., Kress, J.W. "Practical cone-beam algorithm", Journal of the Optical Society of America A, 1(6), 612-619 (1984)
[14] Dalstra, M. et al., "Osteonal mineralization patterns in cortical bones studied by synchrotron radiation-based computed microtomography and scanning acoustic microscopy", in Developments in X-ray Tomography IV, edited by U. Bonse, SPIE Vol. 5535, 143-151 (2004)
[15] Beckmann, F., et al., "New developments for synchrotron-radiation-based microtomography at DESY", in Developments in X-ray Tomography V, edited by U. Bonse, SPIE Vol. 6318, 1-11 (2006)
[16] Donath, T., "Quantitative X-ray Microtomography with Synchrotron Radiation", GKSS-Forschungszentrum Bibliothek, Geesthacht, (2007)
[17] Drews S, et al, "Three dimensional characterization of the bone-cartilage interface using micro computed tomography" in Developments in X-ray Tomography VI, edited by Stuart Stock, Proceedings of SPIE Vol. 7078, (2008).
[18] Grunwaldt, J.-D., Beckmann, F. and Baiker, A., "Application of X-ray microtomography in catalysis: A study of shell-impregnated solid catalysts", HASYLAB annual report, www-hasylab.desy.de, (2007).
[19] Kak, A.C., Slaney, M., "Principles of computerized tomographic imaging", New York, IEEE Press, (1988)
[20] Brunke, O., Odenbach, S., Beckmann, F., "Quantitative structure analysis of aluminium foams by means of µCT", Eur. Phys. J. Appl. Phys. 29(73) (2005)
[21] Sakellariou, A., et al., "Developing a virtual materials laboratory", Materials Today 10(12) 44-51 (2007)